

Usefulness of the automated multiband imaging system for EUS-FNA biopsy specimen evaluation in patients with upper gastrointestinal subepithelial lesions

Kosuke Okuwaki¹, Hiroshi Imaizumi¹, Mitsuhiro Kida¹, Hironori Masutani¹, Tomohisa Iwai¹, Masafumi Watanabe¹, Kai Adachi¹, Masayoshi Tadehara¹, Rikiya Hasegawa¹, Seigo Nakatani¹, Takahiro Kurosu¹, Akihiro Tamaki¹, Wasaburo Koizumi¹

¹Department of Gastroenterology, Kitasato University School of Medicine, Sagamihara, Kanagawa, Japan

ABSTRACT

Background and Objectives: Sample isolation processing by stereomicroscopy (SIPS) was recently introduced as an alternative to rapid on-site cytologic evaluation and showed high accuracy for use in pathologic diagnoses. SIPS is a useful, but slightly complicated procedure; therefore, a new, more straightforward method for the objective estimation of the core tissue amount required during the sampling is desirable. We evaluated the usefulness of the automated multiband imaging system (AMUS) for calculating whitish core amounts in EUS-FNA biopsy (EUS-FNAB) samples from patients with subepithelial lesions (SELs). **Methods:** Four EUS-FNAB specimens per patient were obtained from 20 patients with upper gastrointestinal SELs. The correlation between the whitish core amount calculated by AMUS, length of the manually measured whitish cores (stereomicroscopically visible white core [SVWC]), and sample suitability for pathologic evaluation were analyzed. **Results:** We identified 13 patients with gastrointestinal stromal tumors, five with leiomyomas, one with a schwannoma, and one with an ectopic pancreas. The histological diagnostic accuracy was 100%, median SVWC length was 9 mm, and median whitish core area, calculated using AMUS, was 10 mm². SVWC length correlated with whitish core amount ($\rho = 0.81$, $P < 0.01$) and adequacy score ($\rho = 0.54$, $P < 0.01$). Whitish core amount correlated with adequacy score ($\rho = 0.54$, $P < 0.01$). The area under the receiver-operating characteristic curve calculated for whitish core amount with respect to the histological diagnosis was 0.83 ($P < 0.01$; cutoff ≥ 4 mm², sensitivity 98.4%). **Conclusions:** AMUS, a simple on-site verification instrument, is an alternative to SIPS for determining the appropriate SEL tissue sampling quantity with high diagnostic accuracy.

Key words: automated multiband imaging system, EUS, EUS-guided fine-needle aspiration biopsy, histopathology, stereomicroscopy, subepithelial lesions

INTRODUCTION

Upper gastrointestinal subepithelial lesions (SELs) include gastrointestinal stromal tumors (GISTs),

leiomyomas, schwannomas, lipomas, ectopic pancreatic lesions, and neuroendocrine neoplasms.

This is an open access journal, and articles are distributed under the terms of the Creative Commons Attribution-NonCommercial-ShareAlike 4.0 License, which allows others to remix, tweak, and build upon the work non-commercially, as long as appropriate credit is given and the new creations are licensed under the identical terms.

For reprints contact: WKHLRPMedknow_reprints@wolterskluwer.com

How to cite this article: Okuwaki K, Imaizumi H, Kida M, Masutani H, Iwai T, Watanabe M, *et al.* Usefulness of the automated multiband imaging system for EUS-FNA biopsy specimen evaluation in patients with upper gastrointestinal subepithelial lesions. *Endosc Ultrasound* 2022;11:283-90.

Access this article online	
Quick Response Code: 	Website: www.eusjournal.com
	DOI: 10.4103/EUS-D-21-00143

Address for correspondence

Dr. Kosuke Okuwaki, Department of Gastroenterology, Kitasato University School of Medicine, 1-15-1 Kitasato, Minami, Sagamihara, Kanagawa 252-0374, Japan. E-mail: kokuwaki@kitasato-u.ac.jp

Received: 2021-06-10; **Accepted:** 2021-11-30; **Published online:** 2022-03-21

Their characteristics vary, with some having malignant potential, whereas others follow a benign course that does not require surgical resection.^[1] Therefore, obtaining a histologically confirmed diagnosis is important for distinguishing between the different types of SELs and proposing a correct treatment plan. GISTs, derived from the muscularis propria, are the most common type of SELs. These malignant tumors account for up to 3% of all gastrointestinal tumors.^[2] Similarly, leiomyomas and schwannomas are also derived from the muscularis propria.^[3] EUS-guided specimen collection and specific immunohistochemical staining can distinguish GISTs from other tumors. EUS-FNA biopsy (FNAB) is considered as one of the useful diagnostic tools for SELs.

We previously developed a procedure for sample isolation processing by stereomicroscopy (SIPS) to prepare high-quality tissue specimens for EUS-FNAB as an alternative to rapid on-site evaluation (ROSE) and reported that the pathological diagnostic efficacy of EUS-FNAB was significantly improved when the cutoff length for stereomicroscopically visible white cores (SVWCs), obtained using a 22-gauge needle, was ≥ 3.5 mm (sensitivity over 98%) in SELs.^[4,5] In SIPS, specimens obtained by EUS-FNAB are isolated into their respective SVWCs and red components by the evaluator under a stereomicroscope.^[4] Thus, manual SIPS is a useful but slightly complicated procedure; therefore, it is desirable to create a new, more straightforward method for objective estimation of the core tissue amount required during sampling. We recently reported on the usefulness of a new image-processing technology, the automated multiband imaging system (AMUS), for EUS-FNAB in patients with pancreatic cancer.^[6] The results of the whitish core amount calculated by AMUS strongly correlated with SVWC assessments performed manually. Furthermore, the findings on subgroup analysis (isolation group *vs.* no-isolation group) of the adequacy score of the specimen indicated that isolating SVWC and red components, which is a required process in manual SIPS, was not required for AMUS assessment.

As mentioned above, AMUS was effective in diagnosing pancreatic cancer by EUS-FNAB,^[6] but there are no studies on its use in patients with gastrointestinal SELs. Therefore, this study aimed to investigate the correlation between SVWC lengths calculated manually by physicians and the amount of whitish core calculated using AMUS to evaluate the usefulness of AMUS for

EUS-FNAB in patients with upper gastrointestinal SELs derived from the muscularis propria.

SUBJECTS AND METHODS

Study design

In this single-center prospective study, we enrolled consecutive patients who underwent EUS-FNAB for SELs derived from the muscularis propria of the upper gastrointestinal tract at our hospital between January 2019 and November 2019. The inclusion criteria were age ≥ 20 years and the presence of upper gastrointestinal SELs derived from the muscularis propria requiring pathological diagnosis. Patients with abnormal coagulation parameters were excluded. The primary endpoint was the correlation between SVWC length calculated manually by physicians and the amount of whitish core calculated by AMUS. The secondary outcomes included the correlation between SVWC length and the histological adequacy score, the correlation between the whitish core amount and histological adequacy score in the pathological specimens, the cutoff value of the amount of whitish core for histological diagnosis, the sensitivity of EUS-FNAB using the cutoff value, histological diagnostic accuracy, and procedure-related adverse events (AEs).

This study was conducted in accordance with the tenets of the Declaration of Helsinki and was approved by our institutional review board based on ethical, scientific, and medical validity. All patients provided written informed consent prior to participating in the study.

EUS-FNAB

EUS-FNAB was performed without ROSE, using a linear scanning video echoendoscope (GF-UCT260, TGF-260J; Olympus Medical Systems, Tokyo, Japan) and either a 22 G FNA needle (EZ Shot 3 Plus™; Olympus Medical Systems, Tokyo, Japan) or a 22 G FNB needle (Acquire™; Boston Scientific Corp., Marlborough, MA, USA). The therapist chose the puncture needle. Following stylet withdrawal, 10–20 strokes were made with the needle inside the lesion using a 20-mL syringe under negative pressure. Four needle passes were performed for all lesions. In the first two specimens (isolation group), a technician (one of the two designated endoscopists) measured the SVWC length and isolated the SVWC sample and red components according to the protocol

of our previous study.^[3] In the two remaining specimens (no-isolation group), isolation was not performed.

Patients were examined twice for AEs: 3 h after EUS-FNAB sampling and the following morning. The incidence of AEs up to 30 days after EUS-FNAB sampling was evaluated during medical examinations in the outpatient clinic based on established guidelines.^[7]

Automated multiband imaging system and specimen preparation

The EUS-FNAB sample was assessed using AMUS, as shown in Figure 1, as we previously reported.^[6] The automated multiband imaging device provided by Olympus Corporation, a component of the AMUS, is shown in Figure 2. The vermiform sample obtained via EUS-FNAB was sufficiently extended onto a petri dish and was soaked in 10% buffered formalin solution [Figure 3a]. AMUS obtained multiband image data using nine narrow-band lights equipped with a multiband LED light source with peak wavelengths of 405, 430, 465, 505, 545, 600, 630, 660, and 700 nm [Figure 3b]. The whitish core regions in the multiband image were then detected using a segmentation algorithm by eliminating the influence

of various concentrations of blood background and taking advantage of the property by which the spectral absorption rate of blood varies depending on the wavelength of light used to calculate the whitish core quantity (area) [Figure 3c]. Specifically, the spectral transmittance of a pixel was first determined as a multidimensional vector (A). Next, the spectral transmittance of the whitish core and red component, which were the targets of segmentation, were determined as B and C, respectively. Then, the cosine similarities between A and B and between A and C were determined for each pixel. The pixel was classified into the region with the highest similarity to determine whether it belonged to B or C. Finally, the area (number of pixels) of each region was calculated. The SVWCs were measured under a stereomicroscope ($\times 20$ – 40 , SZX10; Olympus Medical Systems, Tokyo, Japan) using a scale on the microscope monitor screen. In the isolation group, the sample was examined in a petri dish where SVWCs and red components were dissected using injection needles under a stereomicroscope. SVWCs and red components were closely aligned on separate filter papers, immersed in vessels containing 10% neutral buffered formalin, then sent for pathological analyses. In the no-isolation group, samples were closely aligned

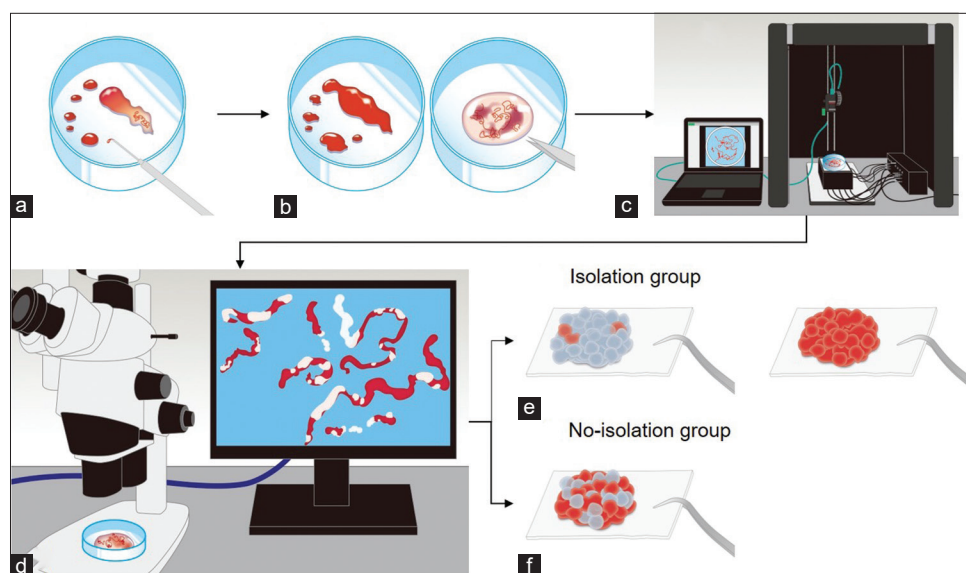


Figure 1. Study outflow. (a) Step 1: The sample in the puncture needle was initially extruded onto the petri dish by compressing air in the syringe and then using a stylet. (b) Step 2: The earthworm-like core sample obtained was immersed in 10% neutral buffered formalin solution under the stereomicroscope. The liquid component remaining after extruding the sample from the needle was sent for cytologic examination. (c) Step 3: The whitish core sample was sufficiently extended onto a petri dish and soaked in 10% buffered formalin solution, irradiated using nine narrow-band lights, and imaged to obtain multiband image data. (d) Step 4: The SVWCs were measured under the stereomicroscope ($\times 20$ – 40 , SZX10; Olympus Medical Systems) using a scale on the microscope monitor screen. (e) Step 5: In the isolation group, the sample in the petri dish was examined, and SVWCs and red components were dissected using injection needles. SVWCs and red components were closely aligned on separate filter papers, immersed in vessels containing 10% neutral buffered formalin, and sent for pathological analyses. (f) Step 6: In the no-isolation group, the samples were closely aligned on filter papers without isolation, immersed in vessels containing 10% neutral buffered formalin, and sent for pathological analyses. AMUS: Automated multiband imaging system; SVWC: Stereomicroscopically visible white core

on filter papers without isolation, immersed in vessels containing 10% neutral-buffered formalin, then sent for pathological analyses.

Pathological examinations

For histological diagnoses, hematoxylin and eosin (HE)-stained specimens were prepared. If immunohistochemical staining was required for diagnosis, it was performed at the discretion of a specialized pathologist. Pathological examinations were performed twice by two or more doctors qualified as specialized pathologists. Among patients who underwent surgical resection following EUS-FNAB, the final diagnosis was considered correct if it was consistent

with the diagnosis from the pathological examination of the resected specimen. For patients with unresected malignancies or benign conditions, the subsequent clinical course was monitored with diagnostic imaging performed. Patients with benign conditions were monitored for ≥ 6 months after EUS-FNAB.

Two gastroenterologists (graduate students in the department of pathology), trained by an expert pathologist and blinded to patient clinical information, assessed each specimen for the histological adequacy score and the degree of blood contamination. The adequacy score and the degree of blood contamination score were classified based on a previously reported scoring system:¹⁸⁾ score 0, samples with no material; score 1, sufficient material for limited cytologic interpretation, but probably representative; score 2, sufficient material for adequate cytologic interpretation, but insufficient for histologic information; score 3, sufficient material for limited histologic interpretation; score 4, sufficient material for adequate histologic interpretation, but a low-quality sample (total material < 1 , $10\times$ power field in length); and score 5, sufficient material for adequate histologic interpretation and a high-quality sample (> 1 , $10\times$ power field in length). The degree of blood contamination was classified as follows: Score 1, significant; score 2, moderate; and score 3, minimal. If the judgments of the two evaluators differed, the one with a lower score was adopted.

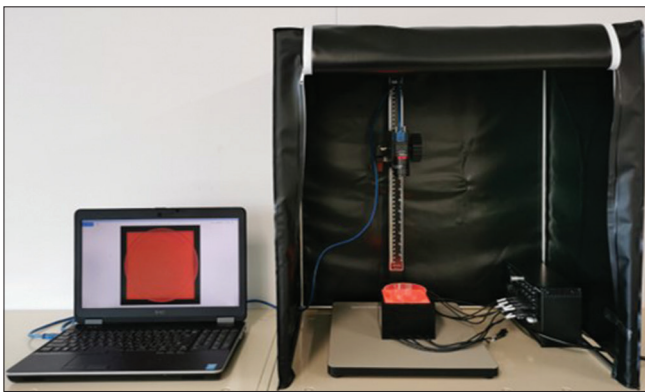


Figure 2. Set-up of the automated multiband imaging device, which is a component of the AMUS. During the actual measurement, the dark curtain was closed, and multiband image data were obtained using nine narrow-band lights. AMUS: Automated multiband imaging system

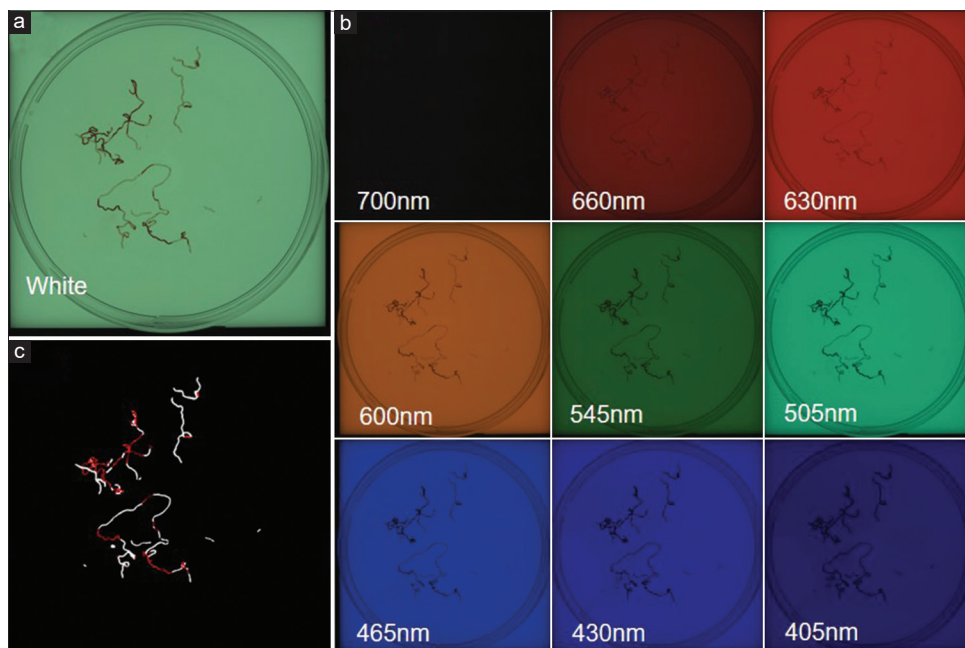


Figure 3. EUS-FNAB samples' images with white light and AMUS. (a) Samples placed in a petri dish and soaked in formalin. (b) AMUS obtained multiband image data using nine narrow-band lights. (c) Whitish core regions in the multiband image, detected using a segmentation algorithm. AMUS: Automated multiband imaging system

Statistical analyses

Power analysis could not be performed because of the study's exploratory nature; therefore, an achievable target of 20 patients (80 specimens) was selected. Receiver-operating characteristic (ROC) curves for the whitish core amount calculated by AMUS for the histological diagnosis were plotted. The accuracy of the area under the curve (AUC) for diagnostic yield was evaluated. The cutoff value required to obtain a histological diagnosis was calculated using the Youden index.^[9] Subgroup analyses were performed for the isolation and no-isolation groups. Statistical comparisons were conducted using the Mann–Whitney *U* test and Fisher's exact probability test for categorical variables, and Spearman's rank correlation coefficient for correlation. Concordance between the classifications of the histological adequacy score and degree of blood contamination determined by the two evaluators was analyzed using the kappa coefficient. Statistical analyses were performed using R statistical package version 3.2.4 (The R. Foundation, Vienna, Austria), with $P < 0.05$, considered statistically significant.

RESULTS

The 20 registered participants included six men and 14 women, with a median age of 67 years (range: 21–87 years). The median lesion's maximum diameter was 25 mm (range, 12–50 mm). Four punctures were performed for each patient, and 80 samples were obtained. Table 1 presents the EUS-FNAB results. FNA needles were selected in three of 20 subjects, of which one was an ectopic pancreas localized in the stomach, one was a GIST localized in the stomach, and one was a GIST localized in the esophagus. GISTs, leiomyomas, schwannomas, and ectopic pancreas lesions were observed in 13, five, one, and one patient(s), respectively. All lesions were diagnosed histologically with immunohistochemical staining except for the ectopic pancreas, which was diagnosed using HE-stained specimens. Throughout the study period, 10 patients with GISTs underwent surgical resection. However, due to serious concomitant disease, three patients with GISTs did not undergo surgical resection. The final diagnoses in the other seven patients with benign diseases (five leiomyomas, one schwannoma, and one ectopic pancreas) were determined by monitoring their clinical courses for >6 months throughout the study duration.

The diagnostic accuracy (per lesion) was not different between the isolation group (95%) and the nonisolation group (100%). In the isolation group, the accuracy, based on histological examination of SVWC, was 95%, which was significantly superior to that of the red components (65%) ($P < 0.01$).

A total of 76 samples (38 from the isolation group and 38 from the no-isolation group) were used for analysis. We excluded the one subject who was diagnosed with ectopic pancreas. Correlations were observed between the SVWC length (median value: 9 mm) calculated manually by physicians and the amount of whitish core calculated by AMUS (median value: 12 mm²) ($\rho = 0.81$, $P < 0.01$); between the SVWC length and the adequacy score (median value score 4) ($\rho = 0.65$, $P < 0.01$); and between the amount of the whitish core and the adequacy score ($\rho = 0.54$, $P < 0.01$).

Table 2 shows the subgroup analysis for the isolation and no-isolation groups. All 76 samples (38 from the isolation group and 38 from the no-isolation group) were used for analysis, excluding the one subject who was diagnosed with ectopic pancreas. The SVWC length, measured according to the study protocol, had a median value of 9 mm (range, 0–99 mm). The median SVWC length was not significantly different between the two groups ($P = 0.42$). Of the 76 samples, 67 (88.2%) met the previously reported cutoff value (SVWC length ≥ 3.5 mm). The sensitivity to histopathological diagnosis using the cutoff value was 98.5% (66/67). The median area of the white core tissue measured was not significantly different between the two groups ($P = 0.09$). The concordance rates, assessed by the kappa coefficient among the evaluators for each sub-classification of the pathological assessment, were 0.60 (95% confidence interval [CI], 0.32–0.87; $P < 0.01$) for the histological adequacy score, and 0.58 (95% CI, 0.38–0.77; $P < 0.01$) for the degree of blood contamination score. There was no significant difference in the median histological adequacy scores between the two groups ($P = 0.37$). The median score of the degree of blood contamination in the isolation group was significantly lower than that in the nonisolation group ($P < 0.01$).

The AUC of the ROC curves calculated for the whitish core concerning the histological diagnosis was 0.83 (95% CI: 0.63–1.04; $P < 0.01$) [Figure 4]. When the cutoff value was set to ≥ 4 mm², the sensitivity of the cutoff value was 98.4%.

Table 1. Results of EUS-FNA biopsy

	All	Isolation group	No-isolation group	P
Technical success, n (%)	20/20 (100)			
Puncture site, n (%)				
Esophagus	1 (5)			
Stomach	18 (90)			
Second portion of the duodenum	1 (5)			
Needle type, n (%)				
FNA needle	3 (15)			
FNB needle	17 (85)			
Final diagnosis, n (%)				
GIST	13 (65)			
Leiomyoma	5 (25)			
Schwannomas	1 (5)			
Ectopic pancreas	1 (5)			
Presence of spindle cells, n (%)	31/80 (39)	12/40 (30)	19/40 (48)	0.17
Accuracy of histological diagnosis, n (%)				
Per pass	76/80 (95)	38/40 (95)	38/40 (95)	1.00
By SVWC		39/40 (95)		
By red components		26/40 (65)		
By none (isolation sample)			38/40 (95)	
Per lesion	20/20 (100)	19/20 (95)	20/20 (100)	1.00
Adverse events, n (%)	0			

The P values (isolation group vs. no-isolation group) were determined using Fisher's exact probability test. FNB: Fine-needle biopsy; GIST: Gastrointestinal stromal tumor; SVWC: Stereomicroscopically visible white core

Table 2. Subgroup analysis between the isolation and no-isolation groups

	All (n=76)	Isolation group (n=38)	No-isolation group (n=38)	P
Length of SVWC median, mm (range)	9 (0-99)	9 (1-99)	9 (0-59)	0.42
Median area of whitish core measured by AMUS, mm ² , (range)	10 (0-75)	12 (1-75)	10 (0-70)	0.09
Median histological adequacy score, (range)	4 (0-5)	4 (2-5)	4 (0-5)	0.37
Median score of the degree of blood contamination, (range)	3 (1-3)	3 (2-3)	2 (1-3)	<0.01

The P values (isolation group vs. no-isolation group) were determined using the Mann-Whitney U test. SVWC: Stereomicroscopically visible white core; AMUS: Automated multiband imaging system

DISCUSSION

In this study of EUS-FNAB for patients with SELs derived from the muscularis propria of the upper gastrointestinal tract, the amount of whitish core calculated by the AMUS strongly correlated with SVWC assessments performed manually. We also demonstrated high sensitivity for histological diagnosis using a cutoff value of ≥ 4 mm².

SIPS, which was devised based on macroscopic on-site evaluation (MOSE), a rapid evaluation method for EUS-FNAB using a 19-gauge needle, was developed by Iwashita *et al.*^[10] SIPS differs from the original MOSE in that it uses a 22-gauge needle, which is frequently used in daily practice, and specimens collected by EUS-FNAB are evaluated using a stereomicroscope rather than grossly by eye. Recently, some usefulness of a modified MOSE using a

22-gauge needle has been reported.^[11-15] However, specimens collected with a 22-gauge needle are thinner than those collected with a 19-gauge needle, and it may be difficult to determine the presence or absence of a whitish core as a result, especially in samples with significant blood contamination. We believe that the advantage of using a stereomicroscope is that it is easier to evaluate the presence and quantity (length) of the whitish core.

In our previous study on the usefulness of SIPS in EUS-FNAB for SEL, the sensitivity of histological diagnosis was over 98% when the SVWC cutoff value (SVWC length ≥ 3.5 mm) was used as an index.^[3,4] However, the evaluation of SVWC was performed by a specific evaluator, and its versatility was unclear. Furthermore, the process of isolating SVWC and red components in the SIPS procedure was complicated and time-consuming.

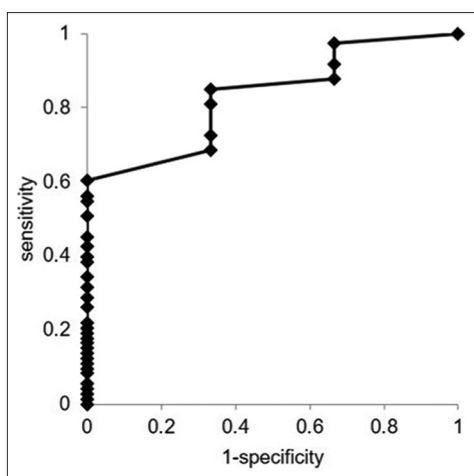


Figure 4. Comparison of core tissue amount measured by the AMUS affecting the histological diagnosis as determined by ROC analysis. The AUC of the ROC curves calculated for the whitish core affecting the histological diagnosis was 0.83 (95% CI: 0.63–1.04; $P < 0.01$). AMUS: Automated multiband imaging system; ROC: Receiver-operating characteristic; AUC: Area under the curve; CI: Confidence interval

Therefore, it was necessary to develop AMUS, a device that could determine the amount of whitish core in correlation with the evaluation of the length of SVWC by a specific evaluator. In addition, by omitting the isolation process, the quality of the specimens can be more easily assessed. We recently reported the usefulness of AMUS in pancreatic cancer and found a high correlation between SVWC measured by specific evaluators and the AMUS-calculated amount of the whitish core.^[6] Based on the results of this study, we found that AMUS showed a high correlation between SVWC measured by specific evaluators and the AMUS-calculated amount of the whitish core in SEL as well as in those with pancreatic cancer.

The findings of the subgroup analysis indicated that by isolating SVWC and red components, a process of SIPS, the degree of blood component contamination in the sample was reduced significantly; however, there were no differences reflected in the adequacy score. We believe this is because SELs are generally packed with tumor cells arranged in an alveolar formation. Once a certain amount of core tissue is obtained, a histopathological diagnosis can be made by confirming positive reactions to disease-specific immunochemical staining. Although isolation can minimize fibrin and blood contamination, it can be concluded that blood contamination does not interfere with the histopathological diagnosis so long as the cutoff value is obtained. The results suggest that the isolation process in SIPS may be omitted.

Despite these favorable results, several limitations of AMUS need to be addressed. First, the process has not been fully automated and requires human intervention. To avoid sample overlapping, the vermiform samples taken by EUS-FNAB must be organized manually onto a petri dish and soaked in formalin solution. If the SVWC is located below overlapping samples, it may not be detected and may be underestimated during multiband image acquisition by the automatic analyzer. Second, AMUS requires adequate equipment preparation. Because it is still in the development stage, we cannot estimate the costs of performing AMUS at this time. Third, given the exploratory nature of this study, a power analysis could not be performed. As only 76 samples were analyzed from 19 subjects in the study, a separate prospective study involving multiple centers and more cases should be conducted to verify the usefulness of AMUS and whether similar results can be obtained from the SIPS process without isolation.

CONCLUSIONS

The SVWC lengths measured manually correlated with the whitish core amount calculated by AMUS. We recommend AMUS as it is simpler than SIPS for EUS-FNAB diagnosis. Our findings may provide useful new indices for EUS-FNAB, particularly in institutions where ROSE cannot be performed. Further multicenter studies are required to validate our findings.

Acknowledgement

We would like to offer our heartfelt thanks go to Mr. Ken Ioka, Mr. Yasuhiro Komiya, Mr. Kazutaka Nishikawa, and Olympus Corporation, who contributed to the development of AMUS, a new image-processing technology that was invaluable throughout the course of our study.

Financial support and sponsorship

This study was supported by a research grant from Olympus Corporation.

Conflicts of interest

Mitsuhiro Kida is an Editorial Board Member of the journal. This article was subject to the journal's standard procedures, with peer review handled independently of this editor and his research groups.

REFERENCES

1. Polkowski M. Endoscopic ultrasound and endoscopic ultrasound-guided fine-needle biopsy for the diagnosis of malignant submucosal tumors.

- Endoscopy* 2005;37:635-45.
2. Goettsch WG, Bos SD, Breekveldt-Postma N, *et al.* Incidence of gastrointestinal stromal tumours is underestimated: Results of a nation-wide study. *Eur J Cancer* 2005;41:2868-72.
 3. Kida M, Kawaguchi Y, Miyata E, *et al.* Endoscopic ultrasonography diagnosis of subepithelial lesions. *Dig Endosc* 2017;29:431-43.
 4. Masutani H, Okuwaki K, Kida M, *et al.* On-site stereomicroscope quality evaluations to estimate white core cutoff lengths using EUS-FNA biopsy sampling with 22-gauge needles. *Gastrointest Endosc* 2019;90:947-56.
 5. Okuwaki K, Masutani H, Kida M, *et al.* Diagnostic efficacy of white core cutoff lengths obtained by EUS-guided fine-needle biopsy using a novel 22G Franseen biopsy needle and sample isolation processing by stereomicroscopy for subepithelial lesions. *Endosc Ultrasound* 2020;9:187-92.
 6. Okuwaki K, Imaizumi H, Kida M, *et al.* New image-processing technology for endoscopic ultrasound-guided fine-needle aspiration biopsy specimen evaluation in patients with pancreatic cancer. *DEN Open* 2022;2:e21.
 7. Cotton PB, Eisen GM, Aabakken L, *et al.* A lexicon for endoscopic adverse events: Report of an ASGE workshop. *Gastrointest Endosc* 2010;71:446-54.
 8. Gerke H, Rizk MK, Vanderheyden AD, *et al.* Randomized study comparing endoscopic ultrasound-guided Trucut biopsy and fine needle aspiration with high suction. *Cytopathology* 2010;21:44-51.
 9. Youden WJ. Index for rating diagnostic tests. *Cancer* 1950;3:32-5.
 10. Iwashita T, Yasuda I, Mukai T, *et al.* Macroscopic on-site quality evaluation of biopsy specimens to improve the diagnostic accuracy during EUS-guided FNA using a 19-gauge needle for solid lesions: A single-center prospective pilot study (MOSE study). *Gastrointest Endosc* 2015;81:177-85.
 11. Leung Ki EL, Lemaistre AI, Fumex F, *et al.* Macroscopic onsite evaluation using endoscopic ultrasound fine needle biopsy as an alternative to rapid onsite evaluation. *Endosc Int Open* 2019;7:E189-94.
 12. Ishiwatari H, Sato J, Fujie S, *et al.* Gross visual inspection by endosonographers during endoscopic ultrasound-guided fine needle aspiration. *Pancreatol* 2019;19:191-5.
 13. Oh D, Seo DW, Hong SM, *et al.* The impact of macroscopic on-site evaluation using filter paper in EUS-guided fine-needle biopsy. *Endosc Ultrasound* 2019;8:342-7.
 14. Kaneko J, Ishiwatari H, Sasaki K, *et al.* Macroscopic on-site evaluation of biopsy specimens for accurate pathological diagnosis during EUS-guided fine needle biopsy using 22-G Franseen needle. *Endosc Ultrasound* 2020;9:385-91.
 15. So H, Seo DW, Hwang JS, *et al.* Macroscopic on-site evaluation after EUS-guided fine needle biopsy may replace rapid on-site evaluation. *Endosc Ultrasound* 2021;10:111-5.